7-2010

Early Signals during CD8+ T Cell Priming Regulate the Generation of Central Memory Cells

Joshua J. Obar
University of Connecticut School of Medicine and Dentistry

Leo Lefrancois
University of Connecticut School of Medicine and Dentistry

Published in final edited form as:
J Immunol. 2010 July 1; 185(1): 263–272. doi:10.4049/jimmunol.1000492.

Early Signals during CD8+ T Cell Priming Regulate the Generation of Central Memory Cells

Joshua J. Obar and **Leo Lefrançois**
Department of Immunology, Center for Integrated Immunology and Vaccine Research, University of Connecticut Health Center, Farmington, CT 06030

Abstract

The $CD8^+$ T cell response to infection is characterized by the appearance of short-lived ($CD127^{low}$ killer cell lectin-like receptor G 1–high) and memory-precursor ($CD127^{high}$ killer cell lectin-like receptor G 1–low) effector cells. How and when central-memory T (T_{CM}; $CD62L^{high}$ $CCR7^+$) cell and effector-memory T(T_{EM}; $CD62L^{low}$ $CCR7^-$) cell subsets are established remains unclear. We now show that the T_{CM} cell lineage represents an early developmental branchpoint during the $CD8^+$ T cell response to infection. Central-memory $CD8^+$ T cells could be identified prior to the peak of the $CD8^+$ T cell response and were enriched in lymphoid organs. Moreover, the kinetics and magnitude of T_{CM} cell development were dependent on the infectious agent. Furthermore, the extent of early Ag availability, which regulated programmed death-1 and CD25 expression levels, controlled the T_{CM}/T_{EM} cell lineage decision ultimately through IL-2 and IL-15 signaling levels. These observations identify key early signals that help establish the T_{CM}/T_{EM} cell dichotomy and provide the means to manipulate memory lineage choices.

In recent years, much has been elucidated regarding how $CD8^+$ T cell responses unfold. Postinfection, extremely rare naive Ag-specific $CD8^+$ T cells (1–3) encounter an APC undergoing an exquisitely orchestrated and somewhat prolonged activation phase (4). Following their activation, Ag-specific $CD8^+$ T cells undergo a rapid expansion, after which only ~5–10% of the pathogen-specific $CD8^+$ T cells are maintained as a memory population. The resulting memory population generally contains increased numbers of Ag-specific $CD8^+$ T cells, compared with the naive pool. These cells exhibit altered homing patterns, increased TCR avidity, and enhanced cytokine production, all of which enable them to respond with increased vigor and potency to future encounters with the same pathogen (5–8).

Questions remain about how, when, and where the decision is made for activated $CD8^+$ T cells to develop into memory cells. A recent study demonstrated that all effector and memory cell populations generated following *Listeria monocytogenes* infection could be generated from a single naive Ag-specific $CD8^+$ T cell (9). Intriguingly, it has been elegantly demonstrated that asymmetric cell division as early as the first cell division can result in proximal and distal daughter $CD8^+$ T cells that have different lineage fates (10). These, and other studies (11), clearly indicate that $CD8^+$ T cells with memory potential are found in the effector CTL pool. Indeed, at the peak of the $CD8^+$ T cell response a small subset of effector cells retain CD127 (IL-7Rα) expression, and these cells go on to form the long-lived memory pool (12,13). Further analyses have demonstrated that the effector $CD8^+$

Address correspondence and reprint requests to Dr. Leo Lefrançois, Department of Immunology, University of Connecticut Health Center, 263 Farmington Avenue, Farmington, CT 06030. llefranc@neuron.uchc.edu.

Disclosures: The authors have no financial conflicts of interest.

T cell population contains both a small population of memory-precursor effector cells (MPECs) and a larger number of terminally differentiated short-lived effector cells (SLECs), distinguished on the basis of CD127 and killer cell lectin-like receptor G1 (KLRG1) expression (14,15).

Additional layers of complexity exist within the memory $CD8^+$ T cell population with respect to phenotype, function, and anatomic location. For example, memory $CD8^+$ T cells are heterogeneous with respect to homing molecule expression and contain at least two distinct populations: $CD62L^{high}$ $CCR7^+$ central-memory T (T_{CM}) cells and $CD62L^{low}$ $CCR7^-$ effector-memory T (T_{EM}) cells (16,17). T_{CM} cells are predominantly found within secondary lymphoid organs, as well as the blood and spleen. In contrast, T_{EM} cells are primarily found within peripheral tissues (i.e., lung, gut, and liver), as well as the blood and spleen (18,19). It is thought that the T_{EM} cell population provides immediate protection at environmental barriers, whereas the T_{CM} cell population provides a second layer of protection upon Ag rechallenge (20). Which memory subset plays a role in mounting a secondary response is dependent, in part, on the location of Ag challenge and characteristics of the pathogen (21–24). Thus, understanding the salient features of memory T cell subsets requires consideration of the parameters of each type of infection or immunization route.

It has been known for some time that $CD8^+$ memory T cell populations gradually shift from being largely $CD62L^{low}$ to primarily $CD62L^{high}$ (25). Two competing hypotheses have been proposed to explain this phenomenon. In the first model, the T_{EM} cell population is largely transient in nature and gives rise to the T_{CM} cell population (21,26); thus far, this effect appears to be the result of abnormally high precursor frequencies used in adoptive transfer systems (1,21,27–29). In the opposing model, the T_{EM} and T_{CM} cell pools, at least based on CD62L expression, are independent lineages with transition of the memory population over time to a predominantly T_{CM} cell phenotype due to the higher homeostatic proliferative rate of T_{CM} cells (1,27). Although previous studies have identified memory precursors present at the peak of the response, the precise origin of the T_{EM} and T_{CM} cell subsets has yet to be elucidated. In this paper, we examined early effector cell (EEC) differentiation events after *L. monocytogenes* and vesicular stomatitis virus (VSV) infection. These studies identify the early origin of the T_{CM} cell population and elucidate the signals required for the development of this subset. These findings appreciably enhance our knowledge regarding the temporal and physical interactions regulating memory $CD8^+$ T cell generation.

Materials and Methods

Mice

Female C57BL/6 and B6-Ly5.2 mice between 5 and 8 wk old were purchased from the National Cancer Institute. Female B6.129S4-*Il2ratm1Dw*/J ($CD25^{-/-}$) mice were purchased from The Jackson Laboratory (Bar Harbor, ME) or were a kind gift from Dr. Charles Surh (Scripps Institute). C57BL/6 IL-$15^{-/-}$ mice (30) were bred in the University of Connecticut Health Center animal facility. All animal protocols were approved by the University of Connecticut Health Center Animal Care Committee.

Generation of bone marrow chimeras

Bone marrow cells were obtained from femurs and tibias of B6.129S4-*Il2ratm1Dw*/J and B6-Ly5.2 mice. Recipient mice were irradiated with ~1000 rads and subsequently injected i.v. with 10^6 bone marrow cells (2:1 ratio of $CD25^{-/-}$/B6). Chimeras were rested 6–8 wk before use in experiments.

Pathogens and infections

Both the rVSV expressing OVA (31) and recombinant *L. monocytogenes* expressing OVA (32) have been previously described. Mice were infected i.v. with either 10^5 PFUs of VSV-OVA or 10^3 CFUs of *L. monocytogenes*-OVA (LM-OVA).

Tissue sample preparation and flow cytometric analysis

Single-cell suspensions were prepared by collagenase digestion, as previously described (18). The H-2K^b tetramer containing either the OVA-derived peptide SIINFEKL or VSV nucleoprotein (VSV-N)-derived peptide RGYVYQGL was generated as previously described (33). Analysis of the Ag-specific CD8$^+$ T cells early postinfection by tetramer enrichment has already been described (1). For general staining, 10^7 lymphocytes per milliliter were incubated with the appropriate peptide: MHC class I tetramers, anti-CD8a (53-6.7; BioLegend, San Diego, CA), and Fc block (2.4G2; BD Pharmingen, San Diego, CA) for 1 h at room temperature. Cells were then washed and stained with anti-CD62L (MEL-14; eBioscience, San Diego, CA), anti-KLRG1 (2F1; Abcam, Cambridge, U.K.), anti-CD127 (A7R34; eBioscience), anti-CD44 (IM7; BioLegend), anti-CD25 (PC-61; BioLegend), anti-PD1 (RPM1-30; BioLegend), and anti-CD11a (2D7; BD Biosciences, San Jose, CA) for 30 min at 4°C. Samples were analyzed on an LSR-II (BD Biosciences), and data analysis was accomplished using FlowJo (Tree Star, Ashland, OR).

Measurement of BrdU incorporation

BrdU was administered to infected mice in their drinking water (0.8 mg/ml). Spleen cells were then cell surface stained as above with SIINFEKL/K^b tetramer, anti-CD8a, anti-CD62L, and anti-CD11a. After this, cells were stained with anti-BrdU according to the BrdU flow kit protocol (BD Biosciences).

Ab blockade of SIINFEKL/K^b

The mAb specific for the OVA derived SIINFEKL peptide presented in the context of H-2K^b (25-D1.16) has been previously described (34). The 25-D1.16 mAb and an isotype-matched irrelevant control Ab (MOPC-21) were purchased from the National Cell Culture Center, and mice were injected i.p. with graded amounts of the 25-D1.16 or control mAb at the indicated times. CD62L expression was quantified at day 7 or day 42 postinfection by flow cytometry, as described above.

Statistical analysis

Statistical significance was determined by either a Student *t* test or ANOVA, using Prism 5 (Graphpad Software). Significance was set at $p < 0.05$.

Results

Kinetics of population conversion toward T_{CM} cells is dependent on infection type

Both VSV and *L. monocytogenes* have been proposed as vaccine vectors, and secondary responses against these pathogens are mediated by distinct memory subsets (23). Given this, we examined CD62L expression after VSV or *L. monocytogenes* infection. At the peak of the CD8$^+$ T cell response, only a few CD62L^{high} cells were detectable in the spleen (Fig. 1A). Over time, CD62L^{high} cells steadily increased within the OVA/K^b-specific CD8$^+$ T cell population (Fig. 1A). Interestingly, OVA/K^b-specific CD8$^+$ T cells induced by *L. monocytogenes* infection had a significantly higher proportion of CD62L^{high} cells when compared with VSV infection at early memory time points. However, by ~125 d postinfection, the frequency of CD62L^{high} cells was similar for both VSV and *L. monocytogenes* infections in the spleen. When the lungs were examined, a similar trend was

observed, although the transition toward CD62L^{high} cells occurred more slowly (Fig. 1A). Within the lymph nodes, emergence of the CD62L^{high} population was rapid. By day 21 postinfection, most *L. monocytogenes*-specific cells were CD62L^{high}, whereas a proportion (~25%) of VSV-specific cells lacked CD62L (Fig. 1A). Thus, *L. monocytogenes* infection, compared with VSV infection, drove more rapid generation of CD62L^{high} central memory cells.

Previous work has indicated that the memory CD8^{+} T cell population transitions from a CD62L^{low} to CD62L^{high} phenotype over time (25). This phenomenon is due to the increased turnover rate of the CD62L^{high} relative to the CD62L^{low} memory cells (1,21,27). As we have just shown, the kinetics of the transition of the memory population from CD62L^{low} to CD62L^{high} differed following VSV and *L. monocytogenes* infection. To determine the mechanism underlying this dichotomy, we compared memory subset proliferation after each infection. VSV-OVA or LM-OVA memory mice were treated with BrdU in their drinking water for 4 wk, and BrdU incorporation into the CD62L^{high} and CD62L^{low} OVA/K^{b}-specific CD8^{+} T cells was quantified. Following either infection, ~40% of the CD62L^{high} memory CD8^{+} T cells had incorporated BrdU (Fig. 1B) and, in both cases, CD62L^{low} memory cells incorporated less BrdU than did CD62L^{high} cells. However, a significantly greater fraction of the CD62L^{low} cells in VSV-primed mice incorporated BrdU, compared with the same subset in *L. monocytogenes*-infected mice (~28% versus ~15%; $p < 0.01$). A greater ratio of CD62L^{high} memory cells incorporating BrdU was observed following *L. monocytogenes* infection versus VSV infection (Fig. 1B), which likely accounts for the delayed transition to a CD62L^{high} memory population following VSV infection. Furthermore, enhanced proliferation of the VSV-specific T_{EM} cell population is likely due to the presence of low-level persistent Ag after VSV infection (35).

T_{CM} cells originate in the memory precursor effector cell population early postinfection

The origin of the CD62L^{high} memory CD8^{+} T cell population remains controversial. Originally, it was postulated that CD62L^{low} cells were capable of re-expressing CD62L, resulting in the gradual generation of the CD62L^{high} memory population (21,26). However, other studies suggest that the CD62L^{high} and CD62L^{low} memory populations are distinct lineages that are not capable of interconverting (1,27). As just discussed, the conversion at the population level of the memory pool toward increased CD62L expression is likely the result of differences in turnover rates between the subsets (1,21,27). Because the effector CD8^{+} T cell population can be subdivided into SLEC and MPEC populations, which are CD127^{low} KLRG1^{high} and CD127^{high} KLRG1^{low}, respectively (14,15), we hypothesized that a proportion of the MPEC population might retain expression of CD62L early postinfection. To test this hypothesis, CD62L expression was quantified on each of the detectable effector cell populations after VSV or *L. monocytogenes* infection. On day 7 postinfection, the MPEC population in the spleen and lymph nodes contained a readily identifiable population of CD62L^{high} cells (Fig. 2A). In contrast, both the SLEC and EEC, which is CD127^{low} KLRG1^{low} in phenotype, populations of OVA/K^{b}-specific CD8^{+} T cells in the spleen, lymph nodes, or lungs largely lacked CD62L expression (Fig. 2A). The EEC population from the lymph nodes did contain a small population of CD62L^{high} cells, but these were extremely few in numbers and may represent cells in transition to the MPEC population. Notably, a greater proportion of the MPECs present after *L. monocytogenes* infection retained CD62L expression (Fig. 2A). In addition, CD62L expression levels of OVA/K^{b}-specific CD8^{+} T cells were tissue specific. Few CD62L^{high} CD8^{+} T cells could be detected in the lung parenchyma, but a much higher frequency of CD62L^{high} CD8^{+} T cells was observed in the lymph nodes (Fig. 2A).

When the kinetics of CD62L^{high} MPEC development in the spleen was examined over time, an interesting pattern emerged. On day 5 postinfection, the frequency of CD62L^{high} cells

was similar between VSV- and *L. monocytogenes*-infected mice (Fig. 2B). Over the next 5 d, the proportion of CD62L^{high} cells declined following both infections, but declined significantly less in mice infected with *L. monocytogenes* (Fig. 2B). Over the next ~4 mo, CD62L^{high} cells increased in the MPEC population at a much greater rate with *L. monocytogenes* infection than with VSV infection, likely as a result of two factors: 1) an early increase in the frequency of CD62L^{high} cells within the MPEC population that is then maintained (Fig. 2A) and 2) the proliferative differences in the T_{EM} cell populations described above (Fig. 1B). Overall, these results shed light on the relationship of the development of the effector cell subsets and the emergence of the CD62L^{high} memory population.

Strength of signal and competition for Ag control T_{CM} cell development

The factors that regulate the generation of the CD62L^{high} and CD62L^{low} memory populations are not well defined. In vitro priming studies suggest that weak stimulation may preferentially generate cells of a T_{CM} cell phenotype, whereas prolonged stimulation will generate T_{EM} phenotype cells (36,37). In vivo, adoptive transfer of graded numbers of TCR transgenic (Tg) CD8$^+$ T cells suggests that increased competition leads to generation of higher numbers of CD62L^{high} cells (21,27,29,38). However, adoptive transfer of high numbers of TCR Tg cells results in a more rapid clearance of *L. monocytogenes* from the spleen and reduced levels of inflammatory cytokines (29,39). Thus, these in vivo studies cannot distinguish between the effects of Ag levels and the inflammatory milieu.

Therefore, we wished to probe whether the CD62L^{high} and CD62L^{low} populations received similar levels of TCR stimulation. Programmed death-1 (PD-1), although functioning as a negative regulator in most cases (40), is rapidly upregulated after TCR engagement (41) or γ_c cytokine signaling (42). We had previously noted that PD-1 expression declined with increased competition using graded numbers of OT-I TCR Tg cells (data not shown). Thus, PD-1 expression at the peak of the CD8$^+$ T cell response appeared to be tunable to the overall strength of stimulation received by the responding cells, which is the sum of TCR, costimulatory, and cytokine signals. Because adoptive transfer of high numbers of TCR Tg cells resulted in weaker PD-1 upregulation and those cells tended to be CD62L^{high}, we next wanted to examine whether PD-1 expression and CD62L expression were related during endogenous CD8$^+$ T cell responses. To test whether this held true in the endogenous CD8$^+$ T cell population, C57BL/6 mice were infected with either VSV-OVA or LM-OVA. At the peak of the OVA/K^b-specific CD8$^+$ T cell response, PD-1 expression was measured on the CD62L^{high} and CD62L^{low} subsets in the lymph nodes (Fig. 3A) and spleen (data not shown). Interestingly, PD-1 expression inversely correlated with CD62L expression. Thus, CD62L^{low} MPEC expressed PD-1, whereas CD62L^{high} MPECs largely lacked PD-1. These data suggested that theCD62L^{high} population had received a weaker overall activation stimulus than did the CD62L^{low} subset.

With the previous PD-1 data in mind, we wanted to directly test the role of TCR triggering and Ag levels on the outcome of endogenous OVA/K^b-specific CD8$^+$ T cells without altering the clearance of the pathogen or inflammatory environment. To achieve this, mice were injected with either graded amounts of 25-D1.16 mAb, which is specific for the OVA-derived SIINFEKL peptide presented in the context of H-2K^b (34), or with an isotype-matched control Ab (MOPC-21). After injection, mice were infected with VSV-OVA, and 7 or 42 d later, OVA/K^b-specific CD8$^+$ T cells in the spleen and lymph nodes were analyzed. In line with the previous observation, injection of increasing amounts of 25-D1.16 mAb resulted in a dose-dependent decrease in PD-1 expression on OVA/K^b-specific MPECs (Fig. 3B). Injection of increasing amounts of the 25-D1.16 mAb also decreased the magnitude of the OVA/K^b-specific CD8$^+$ T cell response (Fig. 4A). Interestingly, 25-D1.16 mAb treatment did not affect the overall distribution of the EEC, MPEC, and SLEC subsets (data

not shown). In contrast, CD62L expression was substantially altered by the injection of the 25-D1.16 mAb (Fig. 4A). Treatment with 250 μg of the 25-D1.16 Ab, but not 50 μg, resulted in a significantly higher proportion of the Ag-specific MPECs expressing CD62L ($p < 0.001$) (Fig. 4A). Furthermore, this difference in CD62L expression was maintained into memory (Fig. 4C). Similar data were obtained using the 25-D1.16 mAb blockade during LM-OVA infection (Fig. 4D). As a control, we also examined the $CD8^+$ T cell response against the VSV-N in the VSV-OVA infected animals and found no differences in the magnitude of the VSV-N/K^b-specific $CD8^+$ T cell response or in the phenotype of the responding cells (Fig. 4B). This finding indicated that the 25-D1.16 mAb did not deplete APC or affect "bystander" responses. Thus, competition for Ag and apparent TCR signal strength regulated not only $CD8^+$ T cell expansion but also T_{CM} cell development.

The timing of naive cell entry into the response has also been proposed to regulate memory development (43). Using adoptive transfer systems, cells added into an ongoing response tend to preferentially form T_{CM}-type memory cells (29,44,45). In addition, the duration of T cell–APC interaction required to drive memory development has been a matter of discussion. Early studies suggested that only a few hours of stimulation with cognate Ag were needed to drive a productive response (46,47), although recent work suggests that a more prolonged period (72–96 h) of Ag availability is required for an optimal T cell response (4,15,48,49). With this in mind, we asked when the CD62L expression pattern was determined. To achieve this, mice were infected with VSV-OVA and treated with 250 μg of the 25-D1.16 mAb at various times. At 7 d postinfection, the OVA/K^b-specific $CD8^+$ T cell response was monitored in the spleen and lymph nodes. Interestingly, effector cell expansion and CD62L expression were differentially regulated. Mice treated with 25-D1.16 mAb just prior to infection had a significantly reduced OVA/K^b-specific $CD8^+$ T cell response, with a greater proportion of the responding OVA/K^b-specific $CD8^+$ T cells being $CD62L^{high}$ (Fig. 5A). Whereas 25-D1.16 mAb blockade as late as 72 h postinfection impaired expansion, mAb-induced modulation of CD62L expression occurred only up to 48 h postinfection and was most notable when mAb was given no later than 24 h postinfection (Fig. 5A). Similarly, during LM-OVA infection, maximal Ag availability for up to 48 h was necessary to induce changes in CD62L regulation, whereas 96 h was needed for optimal expansion (Fig. 5B). Using total numbers of OVA/K^b-specific $CD8^+$ T cells, we also calculated the T_{EM}/T_{CM} cell ratio among MPECs after VSV infection and 25-D1.16 mAb treatment on different days (Fig. 5C). We observed that not only was the overall number of MPECs inhibited by 25-D1.16 treatment early, but also the ratio of T_{EM}/T_{CM} phenotype cells was again skewed toward T_{CM} cells (Fig. 5C). The ratio in control mice was 9.6:1, whereas treatment at day 0 or day 1 decreased the ratio to 2.8:1 and 2:1, respectively. Treatment on days 2 or 3 altered the ratio to ~4:1, but the effect was waning with day 4 treatment (7:1). The magnitude of the effect correlated with the extent of the overall inhibition of the response resulting from Ag blockade. These data demonstrated that the concentration of available Ag during the first 3 d of $CD8^+$ T cell priming was important in regulating CD62L expression, whereas Ag accessibility was necessary for up to 96 h for optimal $CD8^+$ T cell expansion, as previously suggested (4). These data indicated that the T_{CM}/T_{EM} cell lineage choice is made earlier than previously described based on the "latecomer" hypothesis (29,44,45), but does not rule out the possibility of such a phenomenon occurring.

IL-2 and IL-15 signaling play key roles in regulating CD62L expression in vivo

In addition to TCR-mediated signals, cytokines of the γ_c family are also important in memory T cell development and survival (50). Moreover, in vitro studies have demonstrated that IL-2 and IL-15 can generate effector $CD8^+$ T cell populations that resemble T_{EM} and T_{CM} cell populations, respectively (51,52). It was therefore of interest to determine the roles

of these cytokines in memory subset differentiation. CD25 expression by Ag-specific $CD8^+$ T cells was maximal at day 4 postinfection (Fig. 6A). By comparison, alterations of CD62L on the Ag-specific $CD8^+$ T cells following 25-D1.16 mAb administration only occurred when the mAb was administered prior to maximal CD25 expression (Figs. 4, 5). Thus, we tested whether 25-D1.16 mAb administration could alter CD25 levels on the responding Ag-specific $CD8^+$ T cells. Indeed, 4 d after LM-OVA infection, Ag-specific $CD8^+$ T cells expressed high levels of CD25 in the control mice, but cells from mice treated with 250 μg of 25-D1.16 had substantially lower CD25 levels (Fig. 6B). Thus, the effect of Ag competition could be mediated downstream by cytokines of the γ_c family.

The receptors for both IL-2 and IL-15 share two common receptor subunits, CD122 (IL-2/15rβ) and CD132 (γ_c receptor), and each has unique α-chains to form the high-affinity receptor (50). To test the in vivo role of IL-2 and IL-15 in the generation of the T_{CM} and T_{EM} memory cell subsets, C57BL/6:$CD25^{-/-}$ mixed bone marrow chimeras, IL-$15^{-/-}$ mice, and C57BL/6 mice were infected with LM-OVA. At the peak of the $CD8^+$ T cell response (day 9), splenic OVA/K^b-specific MPECs were analyzed for CD62L expression. At this time, $CD25^{-/-}$ OVA/K^b-specific $CD8^+$ T cells had a significantly increased frequency of $CD62L^{high}$ cells ($p = 0.0325$) (Fig. 6C), whereas in the absence of IL-15, the frequency of $CD62L^{high}$ cells was significantly decreased ($p = 0.0179$) (Fig. 6C). These data extend the prior in vitro studies (51,52) and demonstrated that in vivo IL-2–derived signals promote the downregulation of CD62L and formation of the T_{EM} cell population, whereas IL-15–derived signals promote the expression of CD62L and formation of T_{CM} cells. Because the 25-D1.16 blockade inhibited expression of CD25 on the responding CD8 T cells, we next asked whether 25-D1.16 blockade of Ag presentation and CD25 expression had overlapping functions in regulating CD62L expression. For these experiments C57BL/6:$CD25^{-/-}$ mixed bone marrow chimeras were treated with 250 μg of 25-D1.16 or MOPC-21. The mice were then infected with 10^3 CFU of LM-OVA, and the generation of $CD62L^{high}$ T_{CM} cells within the MPEC population on day 9 was analyzed. C57BL/6:$CD25^{-/-}$ mixed bone marrow chimeras treated with MOPC-21 had a low frequency of $CD62L^{high}$ T_{CM} cells in the C57BL/6 compartment and an elevated frequency in the $CD25^{-/-}$ compartment. Interestingly, when the C57BL/6:$CD25^{-/-}$ mixed bone marrow chimeras were treated with 25-D1.16, there was an enhancement of $CD62L^{high}$ T_{CM} cells only of C57BL/6 origin, but not of $CD25^{-/-}$ origin (Fig. 6D). Taken together, these data demonstrated that $CD62L^{high}$ T_{CM} cells are generated when Ag is limiting, and this occurs through the limitation of IL-2–mediated signals.

Discussion

Because immunological memory is the foundation of vaccination, an understanding of the factors regulating the development of the memory population is critical. Furthermore, it has been illustrated that T_{CM} and T_{EM} cells have different recall and protective abilities, depending on the challenge infection (21–24,53). Therefore, understanding the factors governing and regulating the differentiation of the memory subsets is important for generating better vaccines. Strikingly, we have demonstrated that $CD62L^{high}$ $CD8^+$ T cells were mostly found within the MPEC population and could be identified as early as day 5 postinfection (Fig. 2). Furthermore, regulation of CD62L was tied to the overall strength of the activation signal received by the Ag-specific $CD8^+$ T cell early during priming (Figs. 4–6). Our data indicate that the overall potency of the activation signal is, at least in part, the net result of integrating pMHC-TCR engagement and γ_c cytokine signals.

The origin of the memory $CD8^+$ T cell population has long been debated. A recent report from Busch and colleagues (9) elegantly demonstrated that a single naive $CD8^+$ T cell could give rise to all the different subsets of effector and memory $CD8^+$ T cells. Thus, it is critical

to determine the mechanism(s) by which effector cells survive to form the memory population. Furthermore, it is important to understand the relationship of the T_{CM}/T_{EM} cell dichotomy within the different effector $CD8^+$ T cell populations. Earlier work demonstrated that a population of effector $CD8^+$ T cells retains the expression of CD127 (IL-7Rα) (12,13). However, IL-7 signals are not necessary for the survival of that population (54,55). Recent work, using CD127 in combination with KLRG1 expression, has more extensively defined the effector cell populations present during many infections, whereby memory precursor effector cells are defined as $CD127^{high}$ $KLRG1^{low}$ and SLECs are defined as $CD127^{low}$ $KLRG1^{high}$ (14,15,56,57). However, the relationship of the T_{CM}/T_{EM} cell dichotomy was not explored. In this paper, we demonstrate that only when the MPEC population became detectable did $CD62L^{high}$ cells appear. Interestingly, over the next week the frequency of $CD62L^{high}$ OVA/K^b-specific $CD8^+$ T cells actually decreased before slowly shifting to a T_{CM} cell phenotype, as previously described (25). Previous in vitro studies showed that CD62L expression is regulated in a three-step process whereby initial downregulation is mediated by proteolytic cleavage, followed by a rapid re-expression of CD62L and lastly a gradual genetic modulation of CD62L expression (58,59). This three-step model supports our in vivo observations examining the early dynamics of CD62L expression on activated Ag-specific $CD8^+$ T cells. 1) EECs lose cell surface expression of CD62L likely by proteolytic cleavage after initial $CD8^+$ T cell activation; 2) as the immune response continues, heterogeneity within the MPEC population is generated by a small proportion of the Ag-specific $CD8^+$ T cells that are genetically competent to re-express CD62L; and 3) the remainder of the MPECs, as well as EECs and SLECs, undergo epigenetic modification of the CD62L promoter region, prohibiting further gene expression. Thus, memory cell heterogeneity and trafficking patterns originated within the first week of infection. With time, the T_{CM} cell population later dominates the memory pool due to its increased turnover rate, as previously seen (21,27). However, as shown in our work, the rate of conversion differs between pathogens.

The identity of the precise signals that regulate CD62L expression and the differentiation of the T_{CM} cell population in vivo have been unclear. Competition for Ag early in the priming of naive $CD8^+$ T cells will alter the overall signal strength delivered to the responding $CD8^+$ T cells. Previous studies have demonstrated that adoptive transfer of large numbers of TCR Tg $CD8^+$ T cells leads to the generation of more T_{CM} cells (1,21,27,29). This effect is thought to be due to high competition for Ag, but the adoptive transfer of high numbers of TCR Tg $CD8^+$ T cells can also alter the inflammatory milieu owing to rapid clearance of the infection (29,39). Thus, we have used the 25-D1.16 (anti-SIINFEKL/K^b) mAb in a novel manner to specifically limit SIINFEKL/K^b Ag presentation in vivo. Using this method, we have observed two intriguing aspects of $CD8^+$ T cell activation: expansion, and memory differentiation. First, optimal $CD8^+$ T cell expansion required prolonged Ag availability Our previous finding indicates that late APC–T cell interactions form in an Ag-dependent manner (4), and our current data now show that these events enhance T cell expansion. In contrast, restriction of Ag availability only during the first 2–3 d postinfection altered CD62L expression. Therefore, a kinetic dichotomy exists between the requirement for Ag for optimal expansion and CD62L regulation.

One classic consequence of TCR-mediated signaling is the upregulation of CD25 (60). Our data demonstrated that CD25 expression peaked between days 3 and 5 (Fig. 6A) (57,61,62), a time just beyond when 25-D1.16 mAb administration became ineffective at modulating CD62L expression. Indeed, restricting Ag availability limited CD25 expression on the responding Ag-specific $CD8^+$ T cells (Fig. 6B) and also decreased PD-1 expression (Fig. 3B). Furthermore, the observation that the strength of TCR signaling regulates CD25 expression is supported by the fact that vaccination with a weak altered-peptide ligand resulted in diminished CD25 expression on Ag-specific $CD8^+$ T cells (63). In addition, at

least in vitro, high levels of inflammation generated using unmethylated CpG DNA and/or IL-12 can enhance CD25 expression during T cell activation (64). Furthermore, limiting inflammation during *L. monocytogenes* infection by treatment of mice with ampicillin resulted in enhanced T_{CM} cell formation, but the expression of CD25 was not explored (65,66). Interestingly, IL-21 can limit the expression of CD25 on responding $CD8^+$ T cells (67) and enhances CD62L expression (67,68). These results fit well with our observation that IL-2 signaling results in decreased CD62L expression, whereas IL-15 signaling promotes CD62L expression in vivo. Furthermore, limiting Ag availability did not enhance CD62L expression in CD25-deficient cells, suggesting that the regulation of CD62L is ultimately controlled by the levels of IL-2 and IL-15 signaling.

In molecular terms, recent reports have demonstrated that the PI(3)K and mTOR signaling networks play a critical role in regulating T cell migration through control of CD62L, CCR7, and spingosine-1-phospate receptors (52,69). Cantrell and colleagues (52,70) have demonstrated that IL-2 strongly activates the PI(3)K pathway, leading to mTOR activation and the subsequent genetic silencing of CD62L, whereas IL-15 only weakly activates the PI(3)K and mTOR axis and results in the maintenance of CD62L expression. Furthermore, a recent report found that modulating mTOR activity by the administration of low doses of rapamycin, an inhibitor of mTORC1, resulted in an enlarged memory population, which more rapidly became central-memory in phenotype (71). Administration of rapamycin appears to be working by enhancing the Eomes/T-bet ratio (72), which favors memory differentiation (73). Skewing the Eomes/T-bet ratio toward Eomes would likely enhance T_{CM} cell emergence because *Tbx21*$^{-/-}$ $CD8^+$ T cells become $CD62L^{high}$ more rapidly (74). Our in vivo studies using $CD25^{-/-}$ $CD8^+$ T cells and IL-$15^{-/-}$ mice affirm previous in vitro studies examining the ability of IL-2 and IL-15 to support the differentiation of T_{EM}- and T_{CM}-like $CD8^+$ T cell populations, respectively (51,52). In addition, a recent report similarly found that $CD25^{low}$ effector $CD8^+$ T cells preferentially became T_{CM} cells (62). IL-2 could be working through the Blimp1/Bcl6 axis, as *Prdm1*$^{-/-}$ $CD8^+$ T cells acquire a $CD62L^{high}$ phenotype more rapidly (75), whereas $Bcl6^{-/-}$ $CD8^+$ T cells have a decreased frequency of T_{CM} cells (76). Furthermore, high levels of IL-2 are known to enhance Blimp1 expression while repressing Bcl6 expression in vitro (64). $CD4^+$ T cell help is also known to result in decreased CD62L expression on Ag-specific $CD8^+$ T cells (77). We hypothesize that this effect is likely due to IL-2 production by the “helping” $CD4^+$ T cells (57,78), which will then modulate CD62L expression. Our data demonstrated a heretofore unappreciated linkage between Ag availability and IL-2/IL-15 cytokines in the regulation of CD62L expression.

In summary, our results demonstrated that the differentiation of effector and memory $CD8^+$ T cell populations occurred very early in the immune response to pathogens. At these early time points, signals generated by TCR engagement, costimulatory molecules, and the cytokine milieu are integrated by the responding $CD8^+$ T cells to shape the development of effector and memory subsets. Thus, a thorough understanding of the early inflammatory environment and the cellular sources generating this environment will play a critical role in understanding the development of immunological memory.

Acknowledgments

We thank Dr. Charles Surh (The Scripps Institute) for providing CD25-deficient bone marrow. We thank Drs. Evan Jellison and Brian Sheridan for critically reading the manuscript and Kristina Gumpenberger and Quynh-Mai Pham for expert technical assistance.

This work was supported by National Institutes of Health Grants AI41576, AI76457, P01 AI56172 (to L.L.), and F32AI074277 (to J.J.O.).

References

1. Obar JJ, Khanna KM, Lefrançois L. Endogenous naive CD8+ T cell precursor frequency regulates primary and memory responses to infection. Immunity 2008;28:859–869. [PubMed: 18499487]
2. Kotturi MF, Scott I, Wolfe T, Peters B, Sidney J, Cheroutre H, von Herrath MG, Buchmeier MJ, Grey H, Sette A. Naive precursor frequencies and MHC binding rather than the degree of epitope diversity shape CD8+ T cell immunodominance. J Immunol 2008;181:2124–2133. [PubMed: 18641351]
3. Haluszczak C, Akue AD, Hamilton SE, Johnson LD, Pujanauski L, Teodorovic L, Jameson SC, Kedl RM. The antigen-specific CD8+ T cell repertoire in unimmunized mice includes memory phenotype cells bearing markers of homeostatic expansion. J Exp Med 2009;206:435–448. [PubMed: 19188498]
4. Khanna KM, McNamara JT, Lefrançois L. In situ imaging of the endogenous CD8 T cell response to infection. Science 2007;318:116–120. [PubMed: 17916739]
5. Williams MA, Bevan MJ. Effector and memory CTL differentiation. Annu Rev Immunol 2007;25:171–192. [PubMed: 17129182]
6. Kaech SM, Wherry EJ. Heterogeneity and cell-fate decisions in effector and memory CD8+ T cell differentiation during viral infection. Immunity 2007;27:393–405. [PubMed: 17892848]
7. Harty JT, Badovinac VP. Shaping and reshaping CD8+ T-cell memory. Nat Rev Immunol 2008;8:107–119. [PubMed: 18219309]
8. Jameson SC, Masopust D. Diversity in T cell memory: an embarrassment of riches. Immunity 2009;31:859–871. [PubMed: 20064446]
9. Stemberger C, Huster KM, Koffler M, Anderl F, Schiemann M, Wagner H, Busch DH. A single naive CD8+ T cell precursor can develop into diverse effector and memory subsets. Immunity 2007;27:985–997. [PubMed: 18082432]
10. Chang JT, Palanivel VR, Kinjyo I, Schambach F, Intlekofer AM, Banerjee A, Longworth SA, Vinup KE, Mrass P, Oliaro J, et al. Asymmetric T lymphocyte division in the initiation of adaptive immune responses. Science 2007;315:1687–1691. [PubMed: 17332376]
11. Bannard O, Kraman M, Fearon DT. Secondary replicative function of CD8+ T cells that had developed an effector phenotype. Science 2009;323:505–509. [PubMed: 19164749]
12. Schluns KS, Kieper WC, Jameson SC, Lefrançois L. Interleukin-7 mediates the homeostasis of naïve and memory CD8 T cells in vivo. Nat Immunol 2000;1:426–432. [PubMed: 11062503]
13. Kaech SM, Tan JT, Wherry EJ, Konieczny BT, Surh CD, Ahmed R. Selective expression of the interleukin 7 receptor identifies effector CD8 T cells that give rise to long-lived memory cells. Nat Immunol 2003;4:1191–1198. [PubMed: 14625547]
14. Joshi NS, Cui W, Chandele A, Lee HK, Urso DR, Hagman J, Gapin L, Kaech SM. Inflammation directs memory precursor and short-lived effector CD8(+) T cell fates via the graded expression of T-bet transcription factor. Immunity 2007;27:281–295. [PubMed: 17723218]
15. Sarkar S, Kalia V, Haining WN, Konieczny BT, Subramaniam S, Ahmed R. Functional and genomic profiling of effector CD8 T cell subsets with distinct memory fates. J Exp Med 2008;205:625–640. [PubMed: 18316415]
16. Hamann D, Baars PA, Rep MH, Hooibrink B, Kerkhof-Garde SR, Klein MR, van Lier RA. Phenotypic and functional separation of memory and effector human CD8+ T cells. J Exp Med 1997;186:1407–1418. [PubMed: 9348298]
17. Sallusto F, Lenig D, Förster R, Lipp M, Lanzavecchia A. Two subsets of memory T lymphocytes with distinct homing potentials and effector functions. Nature 1999;401:708–712. [PubMed: 10537110]
18. Masopust D, Vezys V, Marzo AL, Lefrançois L. Preferential localization of effector memory cells in nonlymphoid tissue. Science 2001;291:2413–2417. [PubMed: 11264538]
19. Reinhardt RL, Khoruts A, Merica R, Zell T, Jenkins MK. Visualizing the generation of memory CD4 T cells in the whole body. Nature 2001;410:101–105. [PubMed: 11242050]
20. Lefrançois L. Development, trafficking, and function of memory T-cell subsets. Immunol Rev 2006;211:93–103. [PubMed: 16824120]

21. Wherry EJ, Teichgräber V, Becker TC, Masopust D, Kaech SM, Antia R, von Andrian UH, Ahmed R. Lineage relationship and protective immunity of memory CD8 T cell subsets. Nat Immunol 2003;4:225–234. [PubMed: 12563257]
22. Bachmann MF, Wolint P, Schwarz K, Oxenius A. Recall proliferation potential of memory CD8+ T cells and antiviral protection. J Immunol 2005;175:4677–4685. [PubMed: 16177115]
23. Klonowski KD, Marzo AL, Williams KJ, Lee SJ, Pham QM, Lefrançois L. CD8 T cell recall responses are regulated by the tissue tropism of the memory cell and pathogen. J Immunol 2006;177:6738–6746. [PubMed: 17082587]
24. Liu L, Zhong Q, Tian T, Dubin K, Athale SK, Kupper TS. Epidermal injury and infection during poxvirus immunization is crucial for the generation of highly protective T cell-mediated immunity. Nat Med 2010;16:224–227. [PubMed: 20081864]
25. Tripp RA, Hou S, Doherty PC. Temporal loss of the activated L-selectin-low phenotype for virus-specific CD8+ memory T cells. J Immunol 1995;154:5870–5875. [PubMed: 7538535]
26. Sarkar S, Teichgräber V, Kalia V, Polley A, Masopust D, Harrington LE, Ahmed R, Wherry EJ. Strength of stimulus and clonal competition impact the rate of memory CD8 T cell differentiation. J Immunol 2007;179:6704–6714. [PubMed: 17982060]
27. Marzo AL, Klonowski KD, Le Bon A, Borrow P, Tough DF, Lefrançois L. Initial T cell frequency dictates memory CD8+ T cell lineage commitment. Nat Immunol 2005;6:793–799. [PubMed: 16025119]
28. Badovinac VP, Harty JT. Manipulating the rate of memory CD8+ T cell generation after acute infection. J Immunol 2007;179:53–63. [PubMed: 17579021]
29. van Faassen H, Saldanha M, Gilbertson D, Dudani R, Krishnan L, Sad S. Reducing the stimulation of CD8+ T cells during infection with intracellular bacteria promotes differentiation primarily into a central (CD62LhighCD44high) subset. J Immunol 2005;174:5341–5350. [PubMed: 15843531]
30. Kennedy MK, Glaccum M, Brown SN, Butz EA, Viney JL, Embers M, Matsuki N, Charrier K, Sedger L, Willis CR, et al. Reversible defects in natural killer and memory CD8 T cell lineages in interleukin 15-deficient mice. J Exp Med 2000;191:771–780. [PubMed: 10704459]
31. Kim SK, Reed DS, Olson S, Schnell MJ, Rose JK, Morton PA, Lefrançois L. Generation of mucosal cytotoxic T cells against soluble protein by tissue-specific environmental and costimulatory signals. Proc Natl Acad Sci USA 1998;95:10814–10819. [PubMed: 9724787]
32. Pope C, Kim SK, Marzo A, Masopust D, Williams K, Jiang J, Shen H, Lefrançois L. Organ-specific regulation of the CD8 T cell response to *Listeria monocytogenes* infection. J Immunol 2001;166:3402–3409. [PubMed: 11207297]
33. Altman JD, Moss PAH, Goulder PJR, Barouch DH, McHeyzer-Williams MG, Bell JI, McMichael AJ, Davis MM. Phenotypic analysis of antigen-specific T lymphocytes. Science 1996;274:94–96. [PubMed: 8810254]
34. Porgador A, Yewdell JW, Deng Y, Bennink JR, Germain RN. Localization, quantitation, and in situ detection of specific peptide-MHC class I complexes using a monoclonal antibody. Immunity 1997;6:715–726. [PubMed: 9208844]
35. Turner DL, Cauley LS, Khanna KM, Lefrançois L. Persistent antigen presentation after acute vesicular stomatitis virus infection. J Virol 2007;81:2039–2046. [PubMed: 17151119]
36. Geginat J, Sallusto F, Lanzavecchia A. Cytokine-driven proliferation and differentiation of human naive, central memory, and effector memory CD4(+) T cells. J Exp Med 2001;194:1711–1719. [PubMed: 11748273]
37. Gett AV, Sallusto F, Lanzavecchia A, Geginat J. T cell fitness determined by signal strength. Nat Immunol 2003;4:355–360. [PubMed: 12640450]
38. Badovinac VP, Haring JS, Harty JT. Initial T cell receptor transgenic cell precursor frequency dictates critical aspects of the CD8(+) T cell response to infection. Immunity 2007;26:827–841. [PubMed: 17555991]
39. Wirth TC, Pham NL, Harty JT, Badovinac VP. High initial frequency of TCR-transgenic CD8 T cells alters inflammation and pathogen clearance without affecting memory T cell function. Mol Immunol 2009;47:71–78. [PubMed: 19195704]
40. Keir ME, Butte MJ, Freeman GJ, Sharpe AH. PD-1 and its ligands in tolerance and immunity. Annu Rev Immunol 2008;26:677–704. [PubMed: 18173375]

41. Agata Y, Kawasaki A, Nishimura H, Ishida Y, Tsubata T, Yagita H, Honjo T. Expression of the PD-1 antigen on the surface of stimulated mouse T and B lymphocytes. Int Immunol 1996;8:765–772. [PubMed: 8671665]
42. Kinter AL, Godbout EJ, McNally JP, Sereti I, Roby GA, O'Shea MA, Fauci AS. The common gamma-chain cytokines IL-2, IL-7, IL-15, and IL-21 induce the expression of programmed death-1 and its ligands. J Immunol 2008;181:6738–6746. [PubMed: 18981091]
43. Sprent J, Tough DF. Lymphocyte life-span and memory. Science 1994;265:1395–1400. [PubMed: 8073282]
44. D'Souza WN, Hedrick SM. Cutting edge: latecomer CD8 T cells are imprinted with a unique differentiation program. J Immunol 2006;177:777–781. [PubMed: 16818730]
45. Catron DM, Rusch LK, Hataye J, Itano AA, Jenkins MK. CD4+ T cells that enter the draining lymph nodes after antigen injection participate in the primary response and become central-memory cells. J Exp Med 2006;203:1045–1054. [PubMed: 16567390]
46. Kaech SM, Ahmed R. Memory CD8+ T cell differentiation: initial antigen encounter triggers a developmental program in naïve cells. Nat Immunol 2001;2:415–422. [PubMed: 11323695]
47. van Stipdonk MJ, Lemmens EE, Schoenberger SP. Naïve CTLs require a single brief period of antigenic stimulation for clonal expansion and differentiation. Nat Immunol 2001;2:423–429. [PubMed: 11323696]
48. Celli S, Lemaître F, Bousso P. Real-time manipulation of T cell-dendritic cell interactions in vivo reveals the importance of prolonged contacts for CD4+ T cell activation. Immunity 2007;27:625–634. [PubMed: 17950004]
49. Blair DA, Lefrançois L. Increased competition for antigen during priming negatively impacts the generation of memory CD4 T cells. Proc Natl Acad Sci USA 2007;104:15045–15050. [PubMed: 17827281]
50. Schluns KS, Lefrançois L. Cytokine control of memory T-cell development and survival. Nat Rev Immunol 2003;3:269–279. [PubMed: 12669018]
51. Manjunath N, Shankar P, Wan J, Weninger W, Crowley MA, Hieshima K, Springer TA, Fan X, Shen H, Lieberman J, von Andrian UH. Effector differentiation is not prerequisite for generation of memory cytotoxic T lymphocytes. J Clin Invest 2001;108:871–878. [PubMed: 11560956]
52. Sinclair LV, Finlay D, Feijoo C, Cornish GH, Gray A, Ager A, Okkenhaug K, Hagenbeek TJ, Spits H, Cantrell DA. Phosphatidylinositol-3-OH kinase and nutrient-sensing mTOR pathways control T lymphocyte trafficking. Nat Immunol 2008;9:513–521. [PubMed: 18391955]
53. Roberts AD, Ely KH, Woodland DL. Differential contributions of central and effector memory T cells to recall responses. J Exp Med 2005;202:123–133. [PubMed: 15983064]
54. Klonowski KD, Williams KJ, Marzo AL, Blair DA, Lingenheld EG, Lefrançois L. Dynamics of blood-borne CD8 memory T cell migration in vivo. Immunity 2004;20:551–562. [PubMed: 15142524]
55. Hand TW, Morre M, Kaech SM. Expression of IL-7 receptor alpha is necessary but not sufficient for the formation of memory CD8 T cells during viral infection. Proc Natl Acad Sci USA 2007;104:11730–11735. [PubMed: 17609371]
56. Rubinstein MP, Lind NA, Purton JF, Filippou P, Best JA, McGhee PA, Surh CD, Goldrath AW. IL-7 and IL-15 differentially regulate CD8+ T-cell subsets during contraction of the immune response. Blood 2008;112:3704–3712. [PubMed: 18689546]
57. Obar JJ, Molloy MJ, Jellison ER, Stoklasek TA, Zhang W, Usherwood EJ, Lefrançois L. CD4+ T cell regulation of CD25 expression controls development of short-lived effector CD8+ T cells in primary and secondary responses. Proc Natl Acad Sci USA 2010;107:193–198. [PubMed: 19966302]
58. Chao CC, Jensen R, Dailey MO. Mechanisms of L-selectin regulation by activated T cells. J Immunol 1997;159:1686–1694. [PubMed: 9257829]
59. Smalley DM, Ley K. L-selectin: mechanisms and physiological significance of ectodomain cleavage. J Cell Mol Med 2005;9:255–266. [PubMed: 15963248]
60. Cantrell DA, Smith KA. Transient expression of interleukin 2 receptors. Consequences for T cell growth. J Exp Med 1983;158:1895–1911. [PubMed: 6606011]

61. Blattman JN, Grayson JM, Wherry EJ, Kaech SM, Smith KA, Ahmed R. Therapeutic use of IL-2 to enhance antiviral T-cell responses in vivo. Nat Med 2003;9:540–547. [PubMed: 12692546]
62. Kalia V, Sarkar S, Subramaniam S, Haining WN, Smith KA, Ahmed R. Prolonged interleukin-2Ralpha expression on virus-specific CD8+ T cells favors terminal-effector differentiation in vivo. Immunity 2010;32:91–103. [PubMed: 20096608]
63. Zehn D, Lee SY, Bevan MJ. Complete but curtailed T-cell response to very low-affinity antigen. Nature 2009;458:211–214. [PubMed: 19182777]
64. Pipkin ME, Sacks JA, Cruz-Guilloty F, Lichtenheld MG, Bevan MJ, Rao A. Interleukin-2 and inflammation induce distinct transcriptional programs that promote the differentiation of effector cytolytic T cells. Immunity 2010;32:79–90. [PubMed: 20096607]
65. Williams MA, Bevan MJ. Shortening the infectious period does not alter expansion of CD8 T cells but diminishes their capacity to differentiate into memory cells. J Immunol 2004;173:6694–6702. [PubMed: 15557161]
66. Badovinac VP, Porter BB, Harty JT. CD8+ T cell contraction is controlled by early inflammation. Nat Immunol 2004;5:809–817. [PubMed: 15247915]
67. Hinrichs CS, Spolski R, Paulos CM, Gattinoni L, Kerstann KW, Palmer DC, Klebanoff CA, Rosenberg SA, Leonard WJ, Restifo NP. IL-2 and IL-21 confer opposing differentiation programs to CD8+ T cells for adoptive immunotherapy. Blood 2008;111:5326–5333. [PubMed: 18276844]
68. Casey KA, Mescher MF. IL-21 promotes differentiation of naive CD8 T cells to a unique effector phenotype. J Immunol 2007;178:7640–7648. [PubMed: 17548600]
69. Fabre S, Carrette F, Chen J, Lang V, Semichon M, Denoyelle C, Lazar V, Cagnard N, Dubart-Kupperschmitt A, Mangeney M, et al. FOXO1 regulates L-Selectin and a network of human T cell homing molecules downstream of phosphatidylinositol 3-kinase. J Immunol 2008;181:2980–2989. [PubMed: 18713968]
70. Cornish GH, Sinclair LV, Cantrell DA. Differential regulation of T-cell growth by IL-2 and IL-15. Blood 2006;108:600–608. [PubMed: 16569767]
71. Araki K, Turner AP, Shaffer VO, Gangappa S, Keller SA, Bachmann MF, Larsen CP, Ahmed R. mTOR regulates memory CD8 T-cell differentiation. Nature 2009;460:108–112. [PubMed: 19543266]
72. Rao RR, Li Q, Odunsi K, Shrikant PA. The mTOR kinase determines effector versus memory CD8+ T cell fate by regulating the expression of transcription factors T-bet and Eomesodermin. Immunity 2010;32:67–78. [PubMed: 20060330]
73. Intlekofer AM, Takemoto N, Wherry EJ, Longworth SA, Northrup JT, Palanivel VR, Mullen AC, Gasink CR, Kaech SM, Miller JD, et al. Effector and memory CD8+ T cell fate coupled by T-bet and eomesodermin. Nat Immunol 2005;6:1236–1244. [PubMed: 16273099]
74. Intlekofer AM, Takemoto N, Kao C, Banerjee A, Schambach F, Northrop JK, Shen H, Wherry EJ, Reiner SL. Requirement for T-bet in the aberrant differentiation of unhelped memory CD8+ T cells. J Exp Med 2007;204:2015–2021. [PubMed: 17698591]
75. Rutishauser RL, Martins GA, Kalachikov S, Chandele A, Parish IA, Meffre E, Jacob J, Calame K, Kaech SM. Transcriptional repressor Blimp-1 promotes CD8(+) T cell terminal differentiation and represses the acquisition of central memory T cell properties. Immunity 2009;31:296–308. [PubMed: 19664941]
76. Ichii H, Sakamoto A, Kuroda Y, Tokuhisa T. Bcl6 acts as an amplifier for the generation and proliferative capacity of central memory CD8+ T cells. J Immunol 2004;173:883–891. [PubMed: 15240675]
77. Sun JC, Bevan MJ. Defective CD8 T cell memory following acute infection without CD4 T cell help. Science 2003;300:339–342. [PubMed: 12690202]
78. Wilson EB, Livingstone AM. Cutting edge: CD4+ T cell-derived IL-2 is essential for help-dependent primary CD8+ T cell responses. J Immunol 2008;181:7445–7448. [PubMed: 19017930]

Abbreviations used in this paper

EEC	early effector cell

KLRG1	killer cell lectin-like receptor G 1
LM-OVA	*Listeria monocytogenes*-OVA
MFI	mean fluorescence intensity
MPEC	memory-precursor effector cell
PD-1	programmed death-1
SLEC	short-lived effector cell
T_{CM}	central-memory T
T_{EM}	effector-memory T
Tg	transgenic
VSV	vesicular stomatitis virus
VSV-N	VSV nucleoprotein

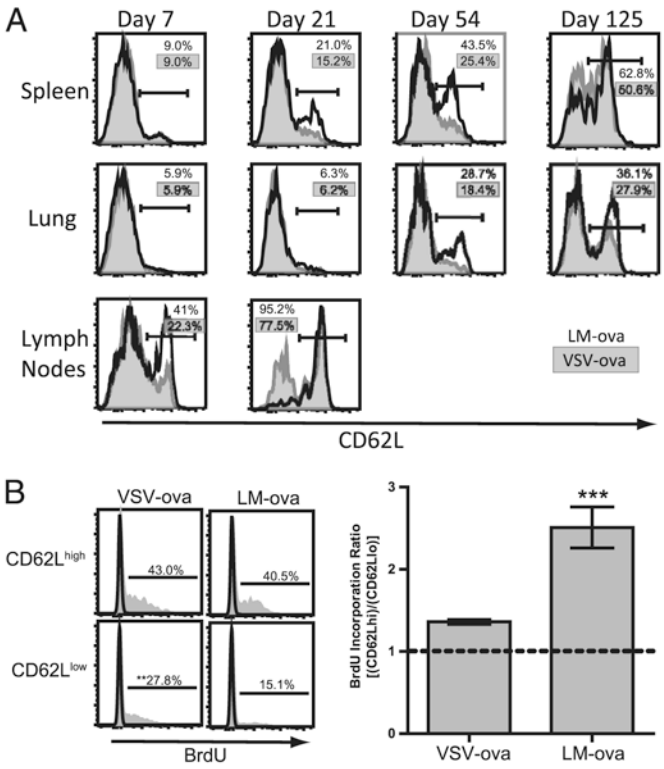

FIGURE 1.

Infection type and turnover rates of T_{EM} cells influence population conversion to T_{CM} cells. *A,* At the indicated times postinfection of C57BL/6 mice with either VSV-OVA or LM-OVA, the OVA/K^b-specific $CD8^+$ T cells in the spleen, lungs, and lymph nodes were monitored for expression of CD62L. Histograms are gated on OVA/K^b-specific $CD8^+$ T cells. The open histograms show CD62L expression after LM-OVA infection and the filled histograms after VSV-OVA infection. Values in the right corner of each histogram represent the mean percentage of $CD62L^{high}$ cells. Each histogram is representative of four or five mice per time-point and three independent experiments. *B,* At 30 d after either VSV-OVA or LM-OVA infection, C57BL/6 mice were given BrdU in their drinking water for 4 wk, at which time BrdU incorporation in OVA/K^b-specific $CD8^+$ T cells in the spleen was determined. Filled histograms show BrdU incorporation in $CD62L^{high}$ or $CD62L^{low}$ OVA/K^b-specific $CD8^+$ T cells, whereas open histograms (dark line) represent an isotype control stain. The graph shows the BrdU incorporation ratio of $CD62L^{high}$ to $CD62L^{low}$ OVA/K^b-specific memory $CD8^+$ T cells. A value >1.0 indicates that more $CD62L^{high}$ memory cells have incorporated BrdU. Each bar represents the mean value of three mice ± one SD. These data are representative of two independent experiments. Statistical significance was determined using a Student *t* test. ***$p < 0.05$.

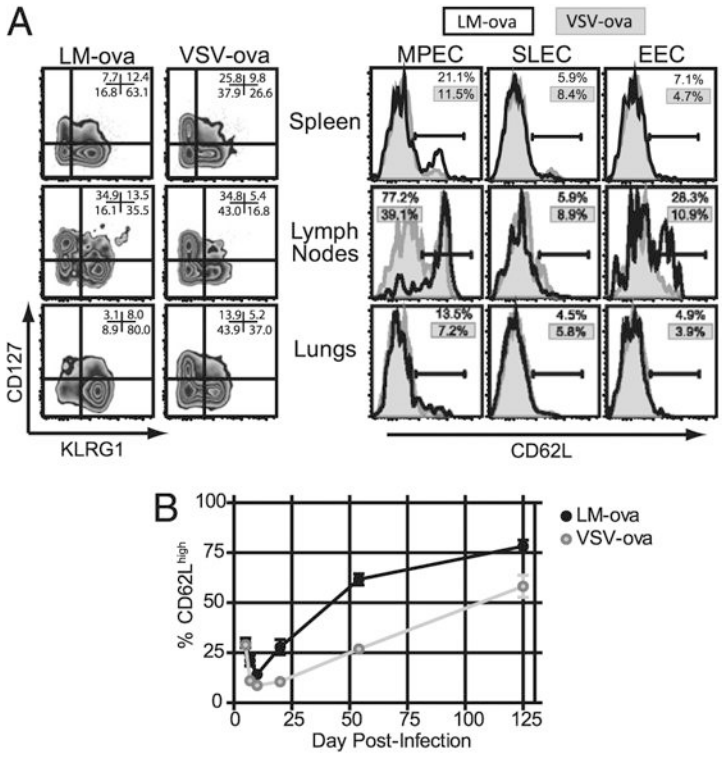

FIGURE 2.

Early postinfection T_{CM} $CD8^+$ T cells are found in the MPEC population. *A*, C57BL/6 mice were infected i.v. with either VSV-OVA or LM-OVA, and 7 d later the OVA/K^b-specific $CD8^+$ T cell population in the spleen, lungs, and lymph nodes was analyzed. Each effector cell subpopulation, based on KLRG1 and CD127 expression, was assessed for CD62L cell surface expression. The zebra plots are gated on the OVA/K^b-specific $CD8^+$ T cells, whereas the histograms are gated on the respective effector cell subpopulations within the Ag-specific subset. The open histograms show CD62L expression after LM-OVA infection and the filled histograms after VSV-OVA infection. Values in the right corner of each histogram represent the mean percentage of $CD62L^{high}$ cells. These data are representative of four or five mice per group and three independent experiments. *B*, Expression kinetics of CD62L after i.v. infection with either VSV-OVA or LM-OVA on the $CD127^{high}$ $KLRG1^{low}$ (MPEC) OVA/K^b-specific $CD8^+$ T cell population was monitored in the spleen. The graph represents the proportion of $CD127^{high}$ $KLRG1^{low}$ OVA/K^b-specific $CD8^+$ T cells expressing CD62L. The data presented are the mean of four or five mice per group ± one SD and is representative of two independent experiments.

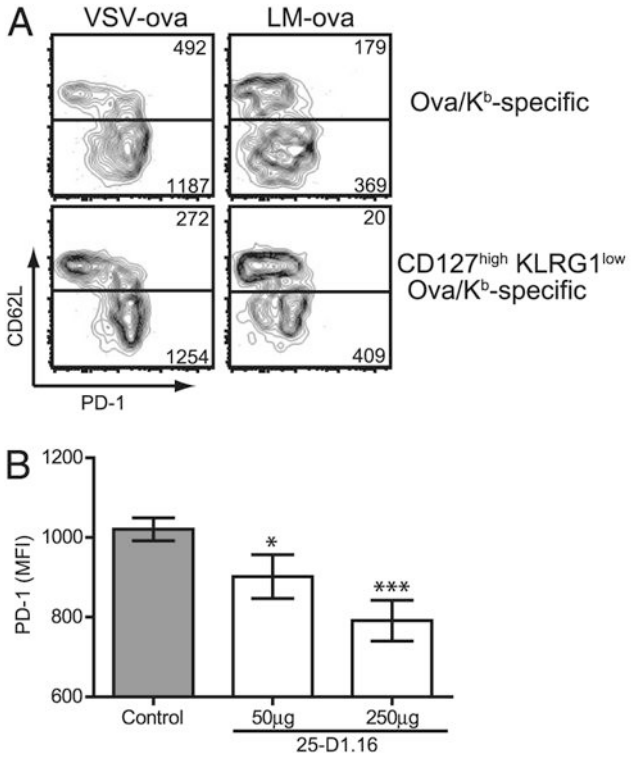

FIGURE 3.

PD-1 expression inversely correlates with CD62L expression of effector cell subsets and is dependent on the strength of TCR engagement. *A*, C57BL/6 mice were infected i.v. with either VSV-OVA or LM-OVA. At 7 d, expression of PD-1 on both $CD62L^{high}$ and $CD62L^{low}$ OVA/K^b-specific $CD8^+$ T cells was monitored in the lymph nodes. Contour plots are representative of four or five mice per group and three independent experiments. The *top panels* are gated on OVA/K^b-specific $CD8^+$ T cells, whereas the *bottom panels* are further gated on the MPEC pool ($CD127^{high}$ $KLRG1^{low}$). Values represent the average MFI of PD-1 staining on the $CD62L^{high}$ and $CD62L^{low}$ populations. Similar data were also obtained from spleen cell analysis. *B*, C57BL/6 mice were treated i.p. with either 50 μg or 250 μg of the 25-D1.16 Ab or 250 μg of a control Ab (MOPC-21), after which the mice were infected i.v. with VSV-OVA. At 7 d, mice were sacrificed, and expression of PD-1 on the OVA/K^b-specific $CD8^+$ T cells was measured in the spleen. The bar graph is a representation of MFI of PD-1 expression on the $CD127^{high}$ $KLRG1^{low}$ (MPEC) OVA/K^b-specific $CD8^+$ T cells. Data are representative of four or five mice per group and two independent experiments. Statistical significance was determined by a one-way ANOVA analysis. ***$p < 0.001$; *$p < 0.05$. MFI, mean fluorescence intensity.

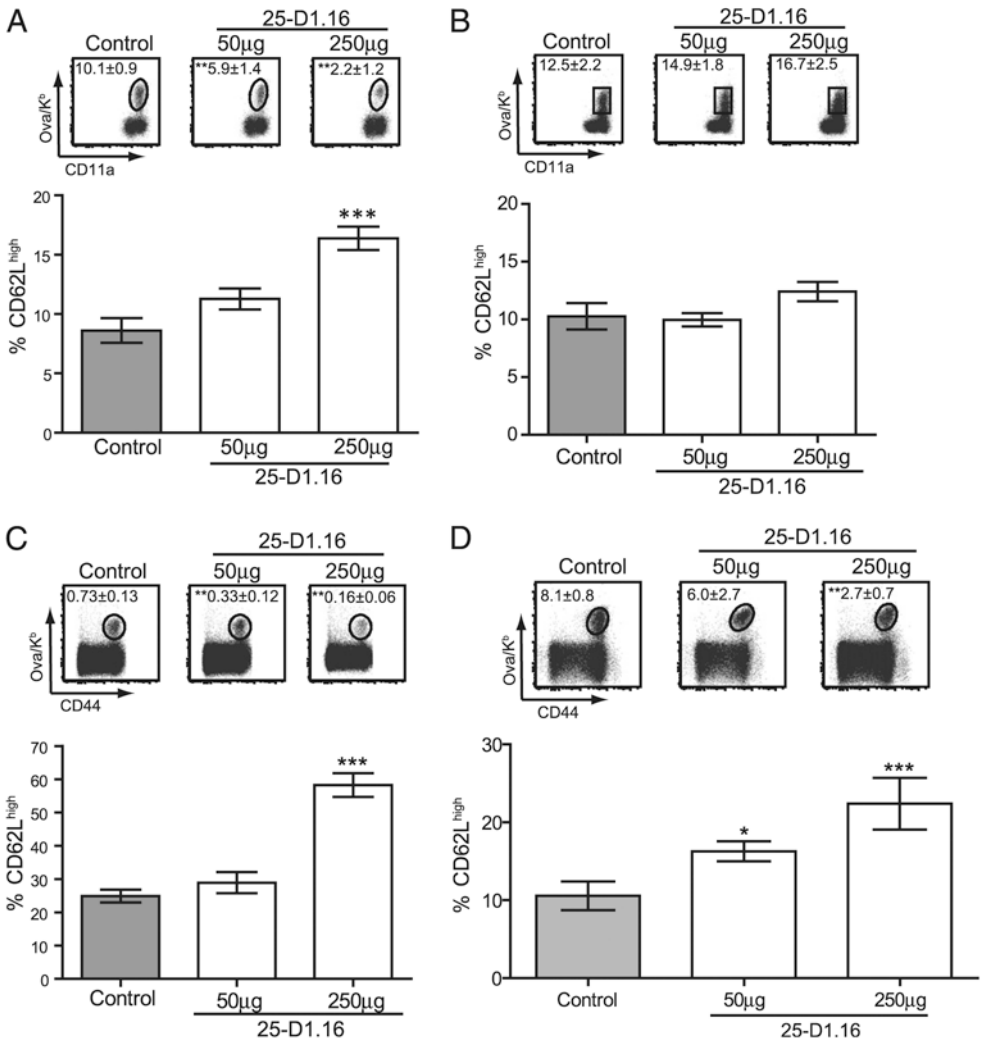

FIGURE 4.

Ag availability during the $CD8^+$ T cell response to infection regulates CD62L expression within the MPEC population. C57BL/6 mice were treated i.p. with either 50 μg or 250 μg of the 25-D1.16 Ab or 250 μg of a control Ab (MOPC-21), after which the mice were infected i.v. with VSV-OVA (*A*–*C*) or with LM-OVA (*D*). At 7 d, the magnitude and phenotype of the OVA/K^b-specific (*A*, *D*) or VSV-N/K^b-specific (*B*) $CD8^+$ T cells were monitored in the spleen. Furthermore, 42 d later, mice were sacrificed, and the magnitude and phenotype of the OVA/K^b-specific $CD8^+$ T cells were monitored in the spleen (*C*). Dot plots are gated on $CD8^+$ T cells. Values represent the group mean ± one SD. The bar graphs are representations of CD62L expression on the $CD127^{high}$ $KLRG1^{low}$ (MPEC) Ag-specific $CD8^+$ T cells. Data are representative of five mice per group and two independent experiments. Similar data were also observed in the lymph nodes. Statistical significance was determined by a one-way ANOVA analysis. ***$p < 0.001$; **$p < 0.01$; *$p < 0.05$.

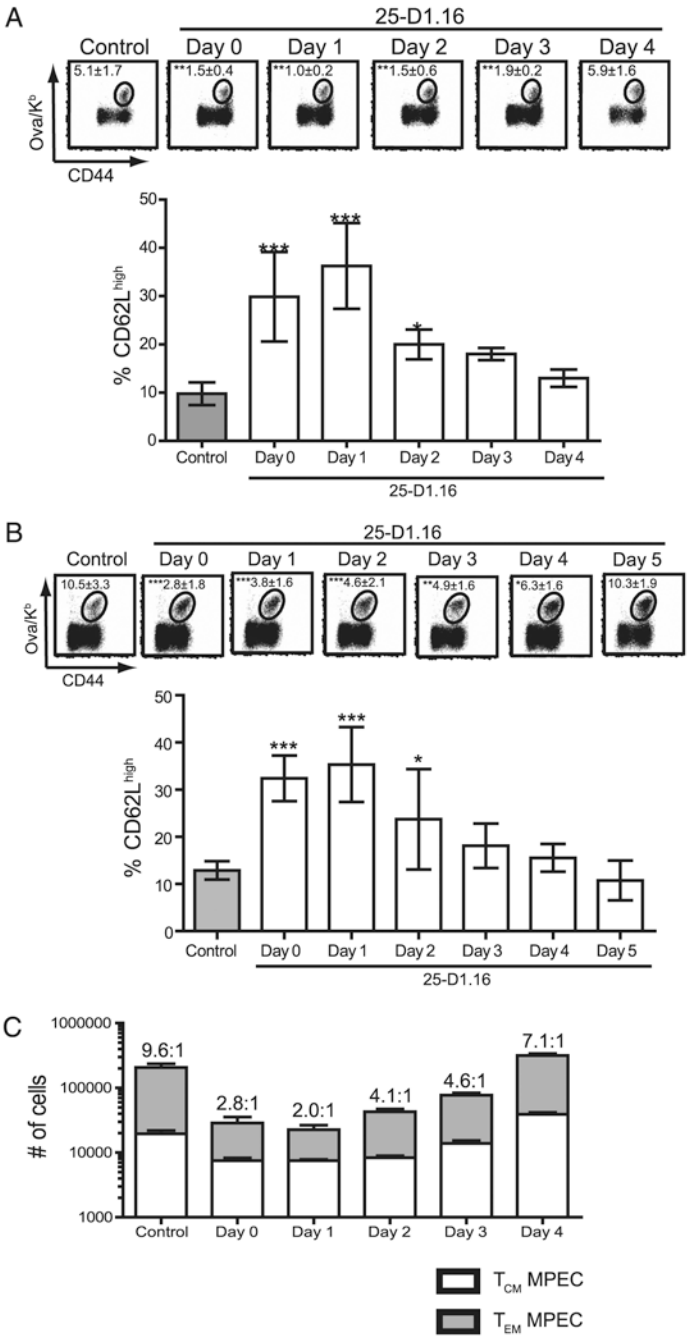

FIGURE 5.

Ag availability early during CD8$^+$ T cell priming regulates CD62L expression within the MPEC population following infection. C57BL/6 mice were treated i.p. with 250 μg of either 25-D1.16 Ab at indicated times or 250 μg of the control Ab (MOPC-21) on day 0. Mice were then infected i.v. with VSV-OVA (*A*, *C*) or LM-OVA (*B*), and 7 d later the OVA/K^b-specific CD8$^+$ T cell population was analyzed in the spleen. Dot plots are gated on CD8$^+$ T cells and display the size of the OVA/K^b-specific CD8$^+$ T cell response. Values represent the group mean ± one SD. The bar graph is a representation of CD62L expression on the CD127^{high} KLRG1^{low} (MPEC) OVA/K^b-specific CD8$^+$ T cells. *C* shows the ratio of CD62L$^-$/CD62L$^+$ cells based on total MPEC numbers. Data are representative of five mice

per group and two independent experiments. Similar data were also observed in the lymph nodes. Statistical significance was determined by a one-way ANOVA analysis. ***$p < 0.001$; **$p < 0.01$; *$p < 0.05$.

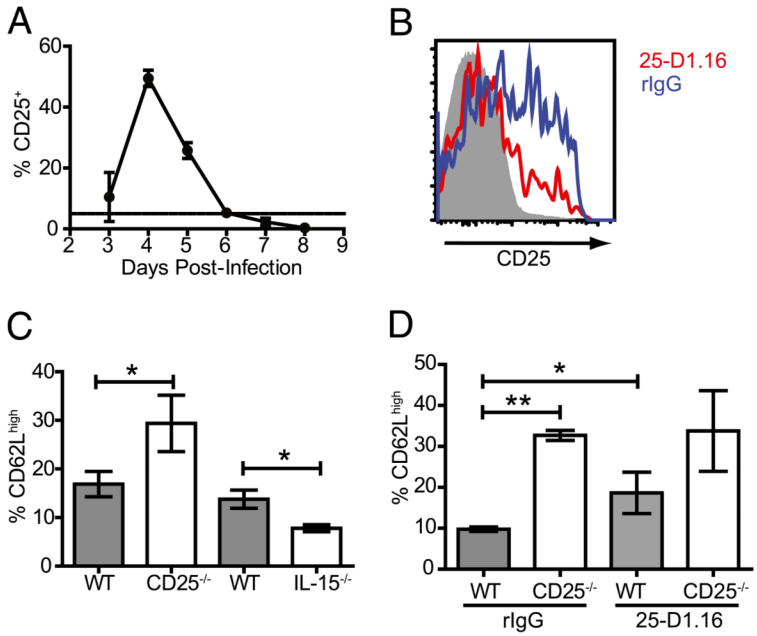

FIGURE 6.

Opposing action of IL-2 and IL-15 signaling on regulation of CD62L expression. *A*, C57BL/6 mice were infected i.v. with 10^3 CFU of LM-OVA. At the indicated times, expression of CD25 on the OVA/K^b-specific $CD8^+$ T cells was quantified in the spleen by tetramer staining. These data are representative of three to five mice per group and two independent experiments. *B*, C57BL/6 mice were treated i.p. with 250 μg of either 25-D1.16 or a control mAb (MOPC-21). After this, mice were infected i.v. with 10^3 CFU of LM-OVA. At 4 d, expression of CD25 on the OVA/K^b-specific $CD8^+$ T cell population in the spleen was analyzed by tetramer enrichment. The filled gray histogram shows CD25 expression on the bulk naive $CD8^+$ T cell population ($CD11a^{low}$ $CD44^{low}$). The open histograms show CD25 expression on the OVA/Kb-specific $CD8^+$ T cells from control mice (blue line) and 25-D1.16-treated mice (red line). These data are representative of three to five mice and four independent experiments. *C*, $CD25^{-/-}$ mixed bone marrow chimeras, C57BL/6, and IL-$15^{-/-}$ mice were infected i.v. with 10^3 CFU of LM-OVA. At 9 d, expression of CD62L on the splenic $CD127^{high}$ $KLRG1^{low}$ (MPEC) OVA/K^b-specific $CD8^+$ T cells was quantified. Data are representative of three to five mice per group and two independent experiments. Statistical significance was measured using a Student *t* test. $*p < 0.05$. *D*, $CD25^{-/-}$ mixed bone marrow chimeras were treated i.p. with 250 μg of either 25-D1.16 or a control mAb (MOPC-21). After this, mice were infected i.v. with 10^3 CFU of LM-OVA. At 9 d, expression of CD62L on the splenic $CD127^{high}$ $KLRG1^{low}$ (MPEC) OVA/K^b-specific $CD8^+$ T cells was quantified. Data are representative of three to five mice per group and two independent experiments. Statistical significance was measured using a Student *t* test. $**p < 0.01$; $*p < 0.05$.